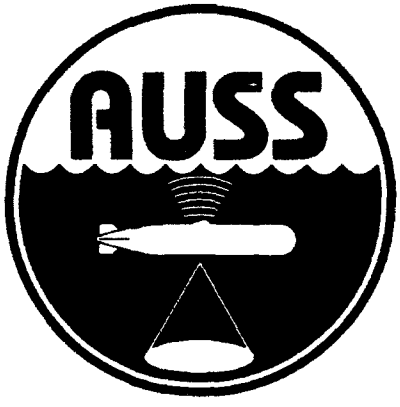

Technical Report 1535
September 1992

Automatic Hovering Algorithms for the Advanced Unmanned Search System (AUSS)

J. L. Held

Technical Report 1535
September 1992

Automatic Hovering Algorithms for the Advanced Unmanned Search System (AUSS)

J. L. Held

NAVAL COMMAND, CONTROL AND OCEAN SURVEILLANCE CENTER
RDT&E DIVISION
San Diego, California 92152-5000

J. D. FONTANA, CAPT, USN
Commanding Officer

R. T. SHEARER
Executive Director

ADMINISTRATIVE INFORMATION

The work reported here was performed for the Assistant Secretary of the Navy, Research and Development (PMO-403), Washington, DC, under program element 0603713N.

Further information on AUSS is available in related reports that represent NRaD efforts through FY 1992. The bibliography is found at the end of this report.

Released by
N. B. Estabrook, Head
Ocean Engineering Division

Under authority of
I. P. Lemaire, Head
Engineering and Computer Sciences Department

SM

EXECUTIVE SUMMARY

OBJECTIVE

Develop and test hovering algorithms for the Advanced Unmanned Search System (AUSS). The AUSS vehicle requires that certain maneuvering functions be performed without human intervention. Among these functions are the hovering functions: hover heading, hover pitch, hover depth, and hover altitude.

APPROACH

The simulation program MatrixX/Systembuild, developed by Integrated Systems, Inc., was used to develop hovering algorithms, and their performance was measured by at-sea testing.

RESULTS

Sea trials showed good agreement with the simulation runs. Simulation played an important role in developing the hover algorithms, which proved successful for use on the AUSS vehicle.

CONTENTS

EXECUTIVE SUMMARY iii

INTRODUCTION 1

HOVERING FUNCTIONS 1

HOVER HEADING 1

HOVER PITCH 2

HOVER DEPTH 2

HOVER ALTITUDE 3

CONCLUSIONS 4

BIBLIOGRAPHY 17

FIGURES

1. Hover heading. 5
2. Hover heading vehicle dynamics. 5
3. Hover heading simulation. 5
4. Heading step response simulation. 6
5. Vehicle hover heading step response. 6
6. Hover pitch. 7
7. Hover pitch vehicle dynamics. 7
8. Hover pitch simulation. 7
9. Pitch step response simulation. 8
10. Vehicle hover pitch step response. 8
11. Hover depth. 9
12. Hover depth vehicle dynamics. 9
13. Hover depth simulation. 10
14. Depth step response simulation. 10
15. Vehicle hover depth step response. 11
16. Hover altitude. 11
17. Altitude filter. 12
18. Hover altitude vehicle dynamics. 12
19. Hover altitude simulation. 12
20. Altitude step response simulation 13
21. Simulated unfiltered output of the altimeter. 13

22. Simulated filtered output of the altimeter. 14
23. Simulated raw altitude data sampled once every 5 seconds. 14
24. Simulated filtered altitude data sampled once every 5 seconds. 15
25. Vehicle hover altitude step response. 15
26. Depth sensor output on altitude step. 16

INTRODUCTION

The Advanced Unmanned Search System (AUSS) was developed by the Naval Command, Control and Ocean Surveillance Center (NCCOSC) to improve the Navy's ability to find and identify items lost or placed on the seafloor at depths as great as 20,000 feet. Items such as the Palomares H-Bomb, the U.S.S. *Scorpion*, the U.S.S. *Thresher*, Korean Airlines Flight 007, Air India Flight 182, and the cargo door of United Airlines Flight 811 are examples of equipment lost by the US and other countries. Searching for these items proved difficult and highlighted a critical technology area: deep ocean search.

The AUSS vehicle requires certain maneuvering functions to be performed without human intervention. Included in these are the hovering functions: hover heading, hover pitch, hover depth, and hover altitude. The simulation program MatrixX/Systembuild, built by Integrated Systems, Inc., was used to develop hovering algorithms, and their performance was measured by at-sea testing. The purpose of this report is to document the design and performance of these algorithms.

HOVERING FUNCTIONS

HOVER HEADING

The block diagram for the hover heading system is shown in figure 1. The controller is a type zero proportional controller with rate feedback. The heading sensor is in the form of a gyrocompass and the rate sensor is a resonant beam device which directly measures yaw rate.

The vehicle dynamics are represented in figure 2. The differential equation models the vehicle as rotary inertia with velocity squared drag, making the system nonlinear.

The simulation block diagram is shown in figure 3. Since the system was anticipated to be "slow" compared to the sample time of approximately 0.5 second, the simulation was done as a continuous system rather than a discrete time system. It was later verified that the output was virtually the same in either case. Since the system was nonlinear, a preliminary goal was that the proportional gain be set so that the vehicle would respond with full moment to a heading error of 0.333 radian or about 19 degrees. This sets $K_p = 3$. A trial and error search for a satisfactory rate feedback yielded a value of $K_r = 20$. This resulted in the nicely damped response shown in figure 4.

Sea trials of the system produced the graph shown in figure 5. There was reasonable agreement with the simulation shown in figure 4 for an initial try, and a very satisfactory response was obtained.

HOVER PITCH

The block diagram for the hover pitch system is shown in figure 6. The controller is a type zero proportional controller with rate feedback. The pitch sensor is in the form of a pendulometer and the rate sensor is a resonant beam device which directly measures pitch rate.

The vehicle dynamics are represented in figure 7. The differential equation models the vehicle as rotary inertia with a righting moment and velocity squared drag, making the system nonlinear.

The simulation block diagram is shown in figure 8. As with the heading, the system was anticipated to be "slow" compared to the sample time of approximately 0.5 second, and the simulation was done as a continuous system rather than a discrete time system. It was later verified that the output was virtually the same in either case. Since the system was nonlinear, a preliminary goal was that the proportional gain be set so that the vehicle would respond with full moment to a pitch error of 0.333 radian or about 19 degrees. This sets $K_p = 3$. A trial and error search for a satisfactory rate feedback yielded a value of $K_r = 20$. This resulted in the nicely damped response shown in figure 9.

Sea trials of the system produced the graph shown in figure 10. There was reasonable agreement with the simulation shown in figure 9 for an initial try, and a very satisfactory response was obtained.

HOVER DEPTH

The block diagram for the hover depth system is shown in figure 11. The controller is a type one proportional controller with rate feedback. The depth sensor is in the form of a pressure transducer and the rate is derived mathematically through a difference equation. The integrator used is limited both positively and negatively and comes off the limit immediately upon reversal of the sign of the error. In addition, the system only operates as a type one when the depth rate is below a certain threshold. This is to prevent overshoot when the vehicle approaches a commanded depth, since the integrator must be prevented from accumulating a large value during the transit time to the set depth. The integrator only comes into play when the vehicle has arrived and has slowed its speed. At this time, the error is integrated up to a value which will offset the buoyancy of the vehicle with the appropriate amount of thrust. The differentiator has a low pass filter in series with it to smooth out noise introduced by the sensor and differentiating process. The filter is a compromise between noise elimination and time delay introduction, which has a destabilizing effect on the system.

The vehicle dynamics are represented in figure 12. The differential equation models the vehicle as inertia and velocity squared drag, making the system nonlinear.

The simulation block diagram is shown in figure 13. Since the system utilizes a mathematical means of generating the derivative of the depth and generally type one systems tend to be less stable, the system was modeled as a discrete system with a sample time of 0.5 second. Since the system was nonlinear, a preliminary goal was that the proportional gain be set so that the vehicle would respond with full thrust to a depth error of 20 feet. This sets $K_p = 0.05$. The integrator gain (K_i) was selected to create a signal which would (over a period of minutes) drive the thrusters to counteract the buoyancy of the vehicle, $K_i = 0.001$. The limit of the integrator is set at ± 1, which will allow for full thrust offset if required. The integrator is enabled when the depth rate falls below ± 0.4 ft/s. This was determined by observing the simulated rate as the vehicle approached the commanded depth. A trial and error search for a satisfactory rate feedback yielded a value of $K_r = 0.8$ with an associated low pass filter time constant of 1.6 seconds. This resulted in the nicely damped response shown in figure 14.

Sea trials of the system produced the graph shown in figure 15. There was reasonable agreement with the simulation shown in figure 14 for an initial try, and a very satisfactory response was obtained.

HOVER ALTITUDE

The block diagram for the hover altitude system is shown in figure 16. The controller is a type one proportional controller with rate feedback. The altitude sensor is in the form of a fathometer measurement which is an output from the Doppler sonar. Being derived from an acoustic sensor, these data are updated relatively slowly (1 second) and have associated noise. In order to improve the data, they are processed by the filter shown in figure 17. The faster update depth sensor with its cleaner signal is used to create a clean altimeter signal. The averaging of the calculated water depth over five samples decreases the noise accordingly, and the information is available at the higher update rate of the depth sensor (0.5 second). The altitude rate is derived mathematically through a difference equation. The integrator used is limited both positively and negatively and comes off the limit immediately upon reversal of the sign of the error. In addition, the system only operates as a type one when the altitude rate is below a certain threshold. This is to prevent overshoot when the vehicle approaches a commanded altitude, since the integrator must be prevented from accumulating a large value during the transit time to the set altitude. The integrator only comes into play when the vehicle has arrived and has slowed its speed. At this time, the error is integrated up to a value which will offset the buoyancy of the vehicle with the appropriate amount of thrust. The differentiator has a low pass filter in series with it to smooth out noise introduced by the sensor and differentiating process. The filter is a compromise between noise elimination and time delay introduction, which has a destabilizing effect on the system.

The vehicle dynamics are represented in figure 18. The differential equation models the vehicle as inertia and velocity squared drag, making the system nonlinear.

The simulation block diagram is shown in figure 19. Since the system utilizes a mathematical means of generating the derivative and generally type one systems tend to be less stable, the system was modeled as a discrete system with a sample time of 1 second. The faster data rate of 0.5 second introduced by the filter was conservatively ignored. Since the system was nonlinear, a preliminary goal was that the proportional gain be set so that the vehicle would respond with full thrust to an altitude error of 20 feet. This sets $K_p = 0.05$. The integrator gain (K_i) was selected to create a signal which would (over a period of minutes) drive the thrusters to counteract the buoyancy of the vehicle, $K_i = 0.001$. The limit of the integrator is set at ± 1, which will allow for full thrust offset if required. The integrator is enabled when the altitude rate falls below ± 0.4 ft/s. This was determined by observing the simulated rate as the vehicle closed the commanded altitude. A trial and error search for a satisfactory rate feedback yielded a value of $K_r = 0.8$ with an associated low pass filter time constant of 1.6 seconds. This resulted in the nicely damped response shown in figure 20.

It is of some interest to examine the performance of the altitude filter. Shown in figure 21 is the simulated unfiltered output of the altimeter. Figure 22 shows the filtered output. The data are processed one more time to simulate the effect of the status display employed on the AUSS. The data are quantized to a resolution of 1 foot and sampled once every 5 seconds. Figure 23 shows the simulated raw altitude data sampled in this manner, and figure 24 shows the simulated filtered data sampled similarly. These outputs can now be compared one to one with figures 25 and 26, which show the actual sea trial data taken by the status display of the altitude and depth sensor data. The apparent agreement of the simulations with actual data indicates that the assumed noise on the altimeter is ± 2 feet rms and that the simulated vehicle response shown in figure 20 must be accurate.

CONCLUSIONS

The hover algorithms have been used successfully on the AUSS. Simulation plays an important role in developing this technology. Future programs should benefit from the information gained in developing the hover algorithms.

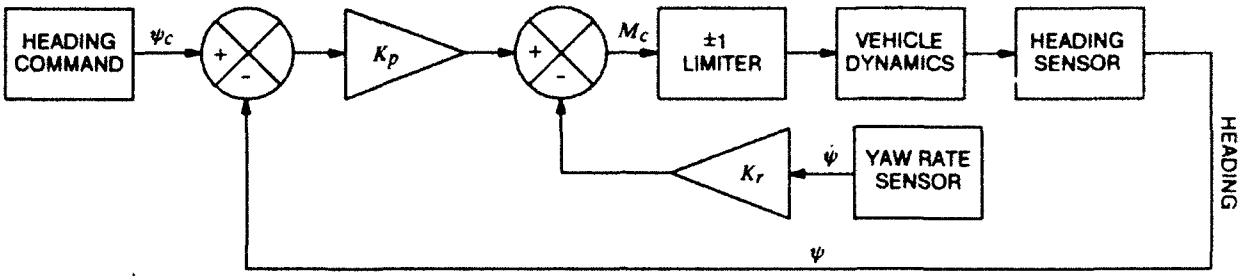

CONTROL EQUATION:

$M_c = K_p(\psi_c - \psi) - K_r\dot{\psi}$

ψ = HEADING
ψ_c = HEADING COMMAND
M_c = MOMENT COMMAND
K_p = PROPORTIONAL GAIN = 3
K_r = RATE FEEDBACK GAIN = 20

Figure 1. Hover heading.

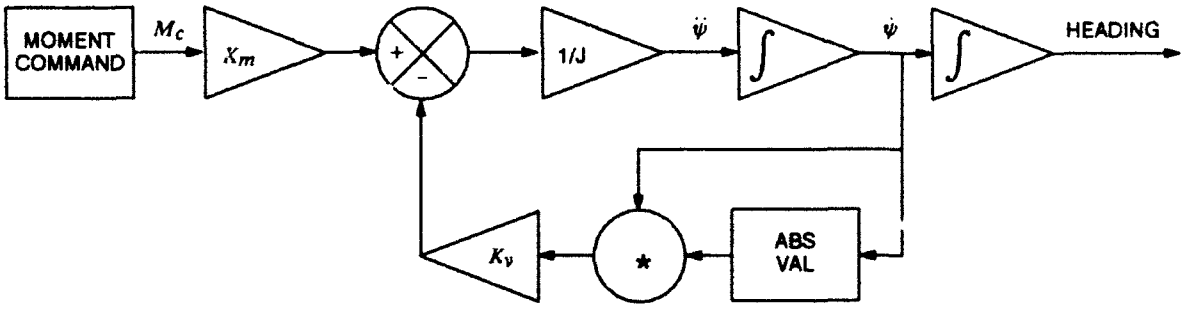

DIFFERENTIAL EQUATION:

$J\ddot{\psi} + K_v\,\dot{\psi}|\dot{\psi}| = K_m M_c$

ψ = HEADING
M_c = MOMENT COMMAND
K_m = MOMENT GAIN = 77 ft-lb
K_v = DRAG CONSTANT = K_v = 1200 ft-lb-s^2
1/J = 1/MOMENT OF INERTIA = 1/J = 0.00028 1/(ft-lb-s^2)

Figure 2. Hover heading vehicle dynamics.

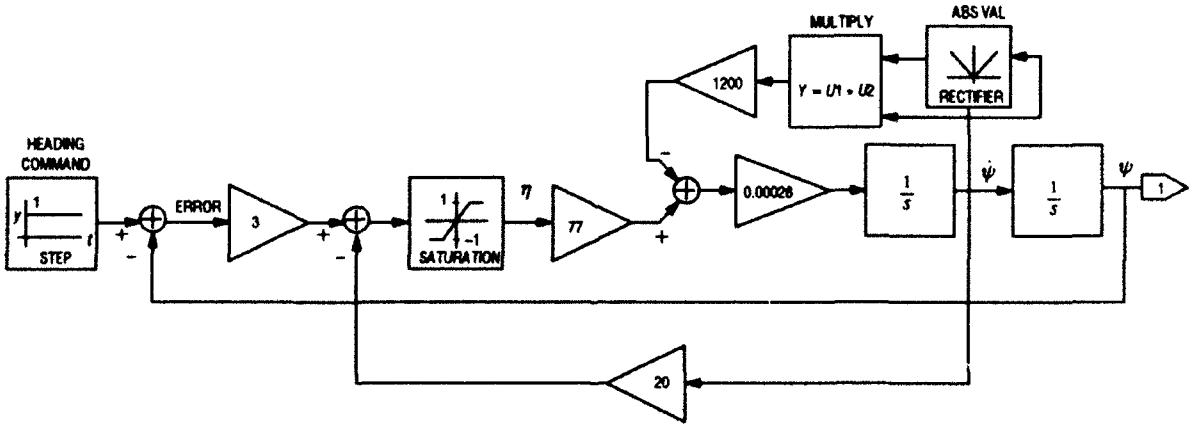

Figure 3. Hover heading simulation.

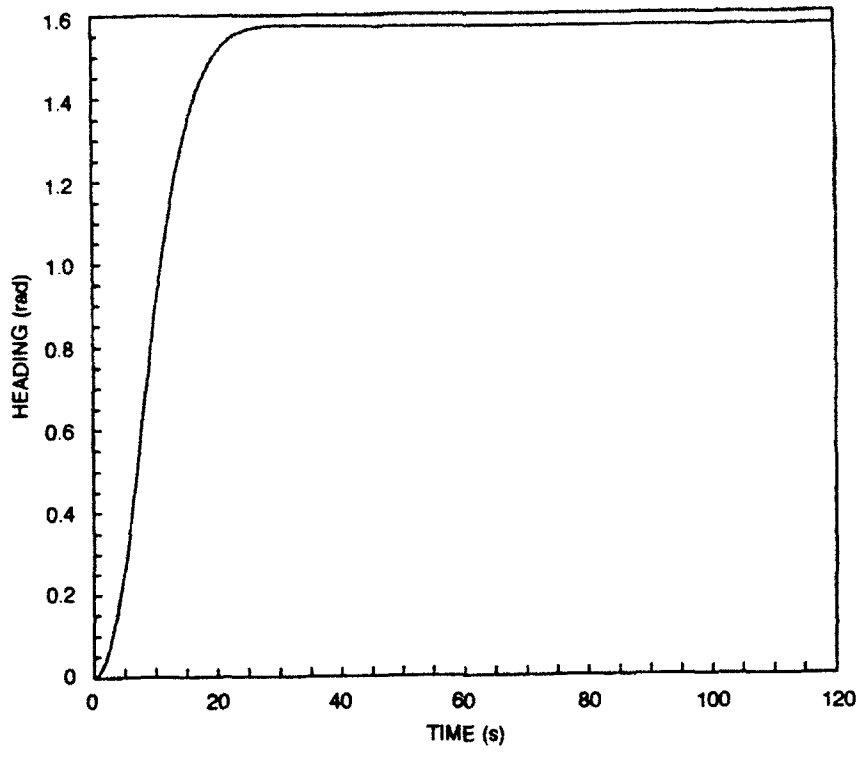

Figure 4. Heading step response simulation.

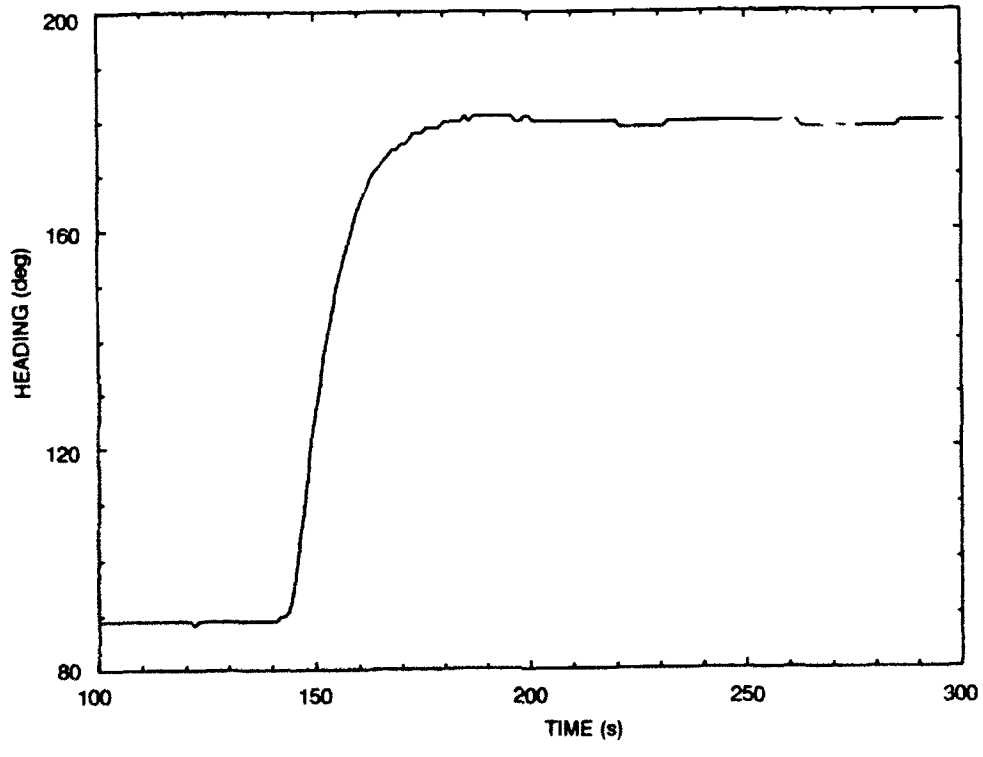

Figure 5. Vehicle hover heading step response.

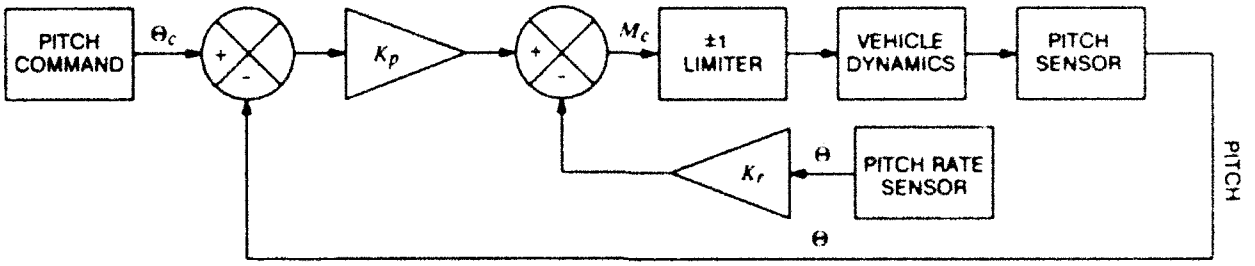

CONTROL EQUATION:
$M_c = K_p(\Theta_c - \Theta) - K_r\dot{\Theta}$

Θ = PITCH
Θ_c = PITCH COMMAND
M_c = MOMENT COMMAND
K_p = PROPORTIONAL GAIN = 3
K_r = RATE FEEDBACK GAIN = 10

Figure 6. Hover pitch.

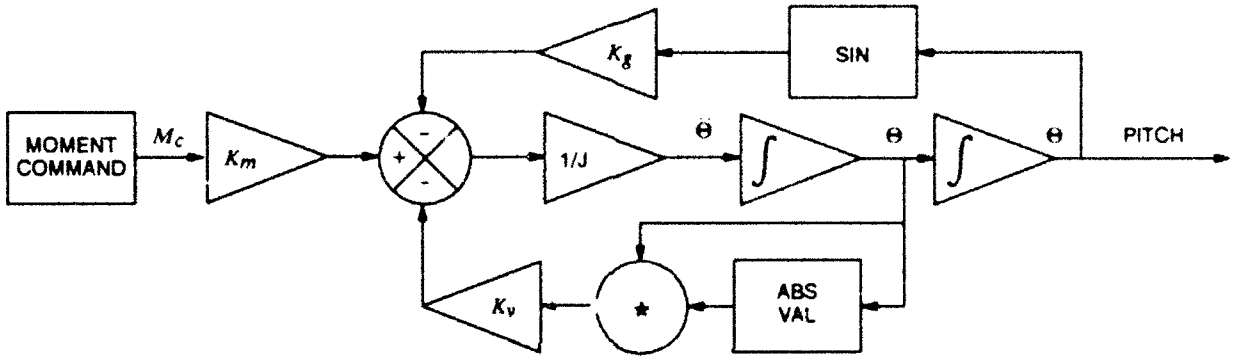

DIFFERENTIAL EQUATION:
$J\ddot{\Theta} + K_v\,\dot{\Theta}|\dot{\Theta}| + K_g \sin\Theta = K_m M_c$

Θ = HEADING
M_c = MOMENT COMMAND
K_m = MOMENT GAIN = 133.7 ft-lb
K_v = DRAG CONSTANT = K_v = 1200 ft-lb-s^2
K_g = CB-CG CONSTANT = K_g = 112.5 ft-lb
1/J = 1/MOMENT OF INERTIA = 1/J = 0.00028 1/(ft-lb-s^2)

Figure 7. Hover pitch vehicle dynamics.

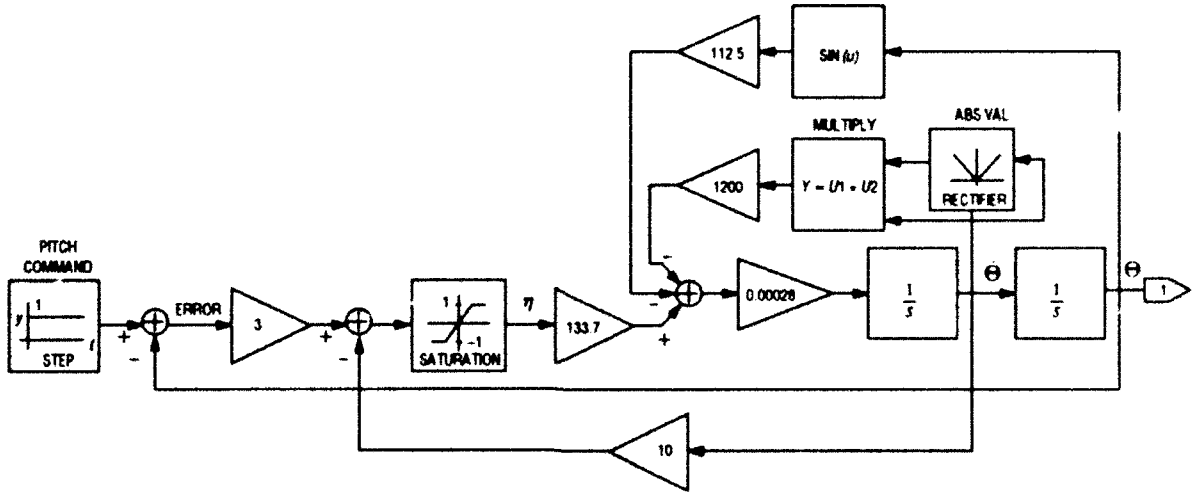

Figure 8. Hover pitch simulation.

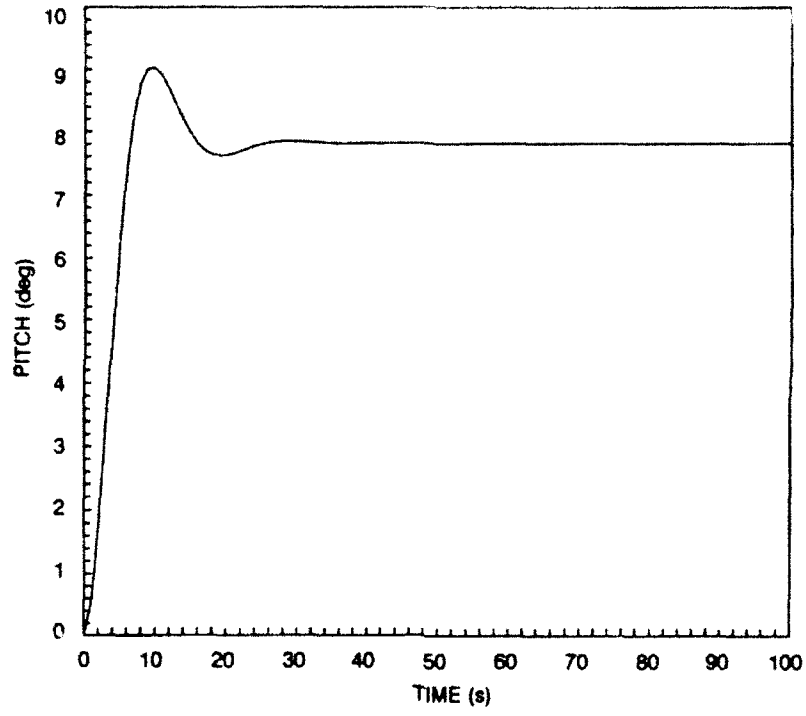

Figure 9. Pitch step response simulation.

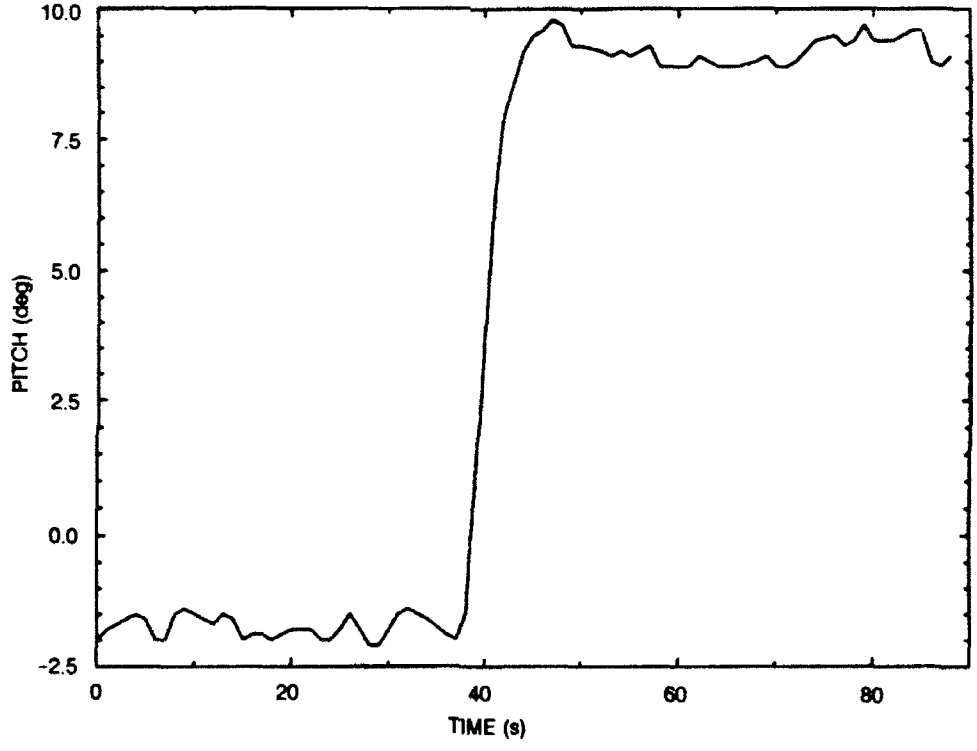

Figure 10. Vehicle hover pitch step response.

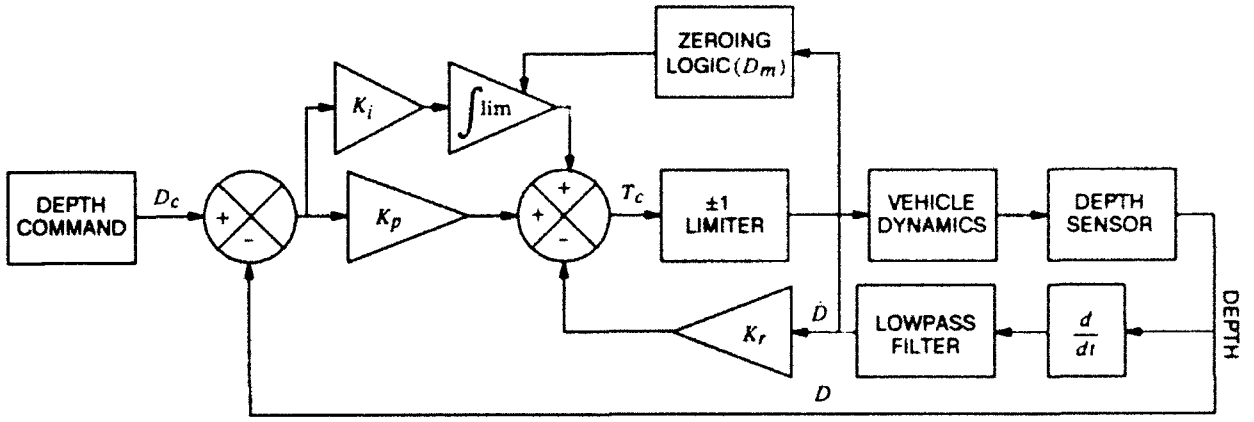

CONTROL EQUATIONS:

$$T_c = K_p(D_c - D) - K_r\dot{D} \quad \text{if } D > \dot{D}_m$$

$$T_c = K_p(D_c - D) - K_r\dot{D} + K_i \int^{\text{lim}} (D_c - D)dt \quad \text{if } D < \dot{D}_m$$

D = DEPTH
D_c = DEPTH COMMAND
$\dot{D}_m$ = DEPTH RATE THRESHOLD = 0.4 ft-s
T_c = THRUST COMMAND
K_p = PROPORTIONAL GAIN = 0.05
K_r = RATE FEEDBACK GAIN = 0.8
K_i = INTEGRATOR GAIN = 0.001
lim = INTEGRATOR LIMIT = ±1
τ = TIME CONSTANT FOR LOW PASS FILTER - 1.6 s

Figure 11. Hover depth.

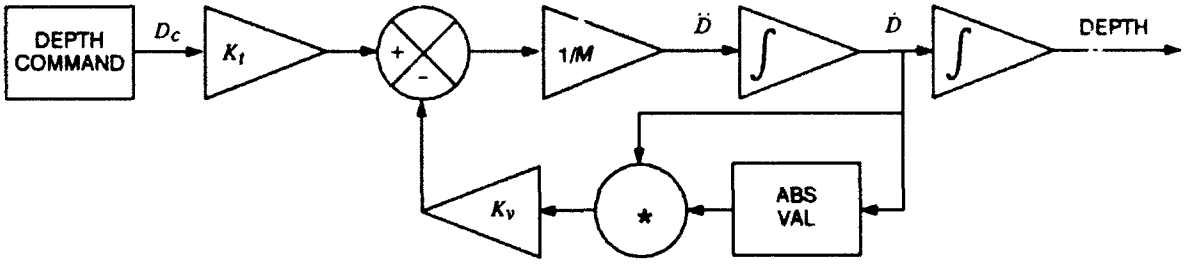

DIFFERENTIAL EQUATION:

$$M\ddot{D} + K_v\,\dot{D}|\dot{D}| = K_tD_c$$

D = DEPTH
D_c = DEPTH COMMAND
K_t = THRUST GAIN = 26 lb
K_v = DRAG CONSTANT = 15.2 lb-s^2/ft^2
1/M = 1/MASS = 0.00367 ft/lb-s^2

Figure 12. Hover depth vehicle dynamics.

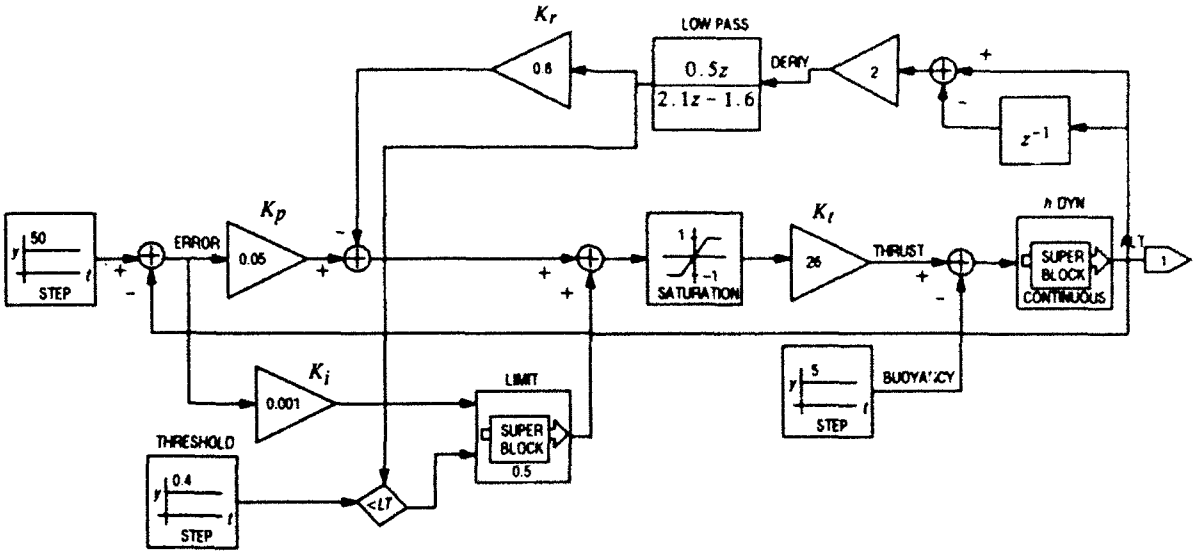

Figure 13. Hover depth simulation.

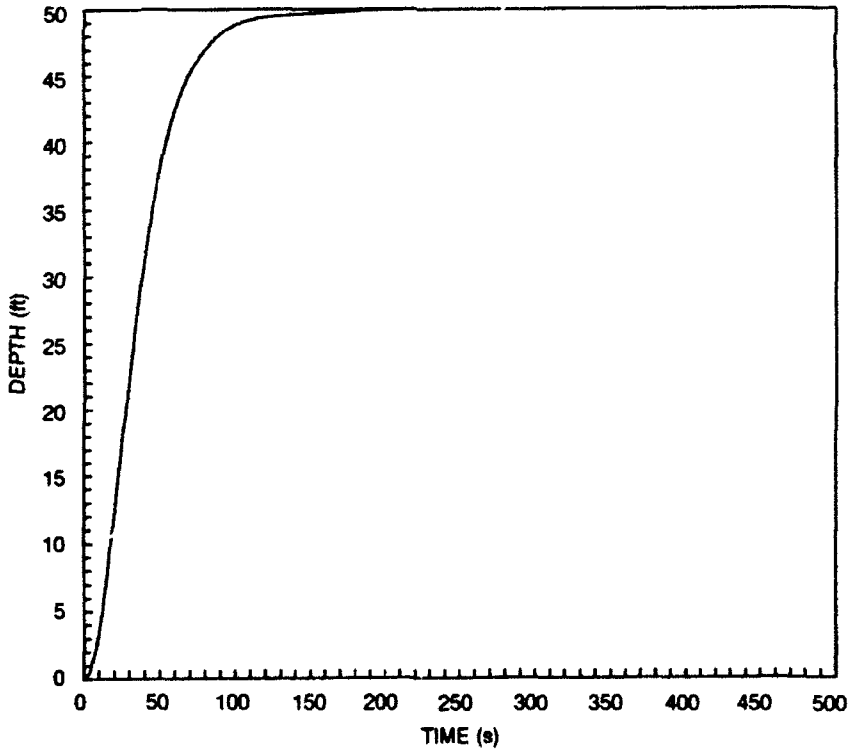

Figure 14. Depth step response simulation.

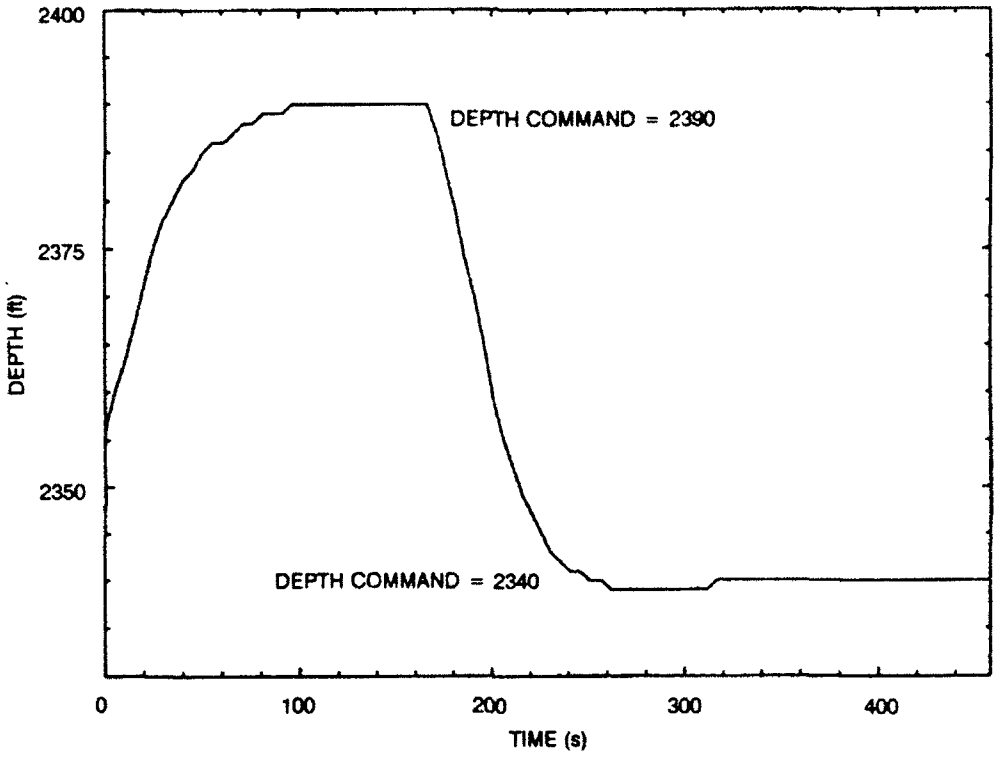

Figure 15. Vehicle hover depth step response.

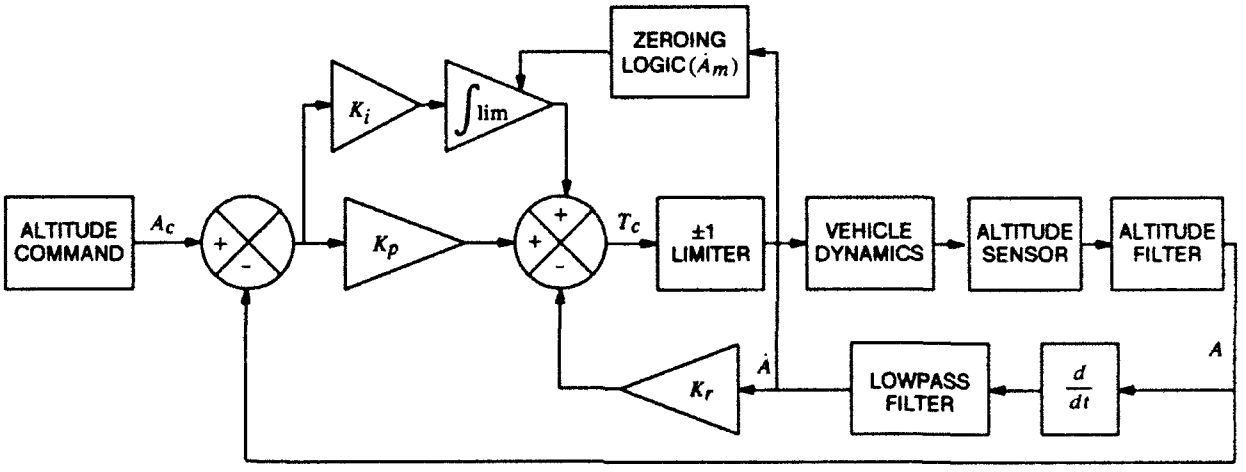

CONTROL EQUATIONS:

$$T_c = K_p(A_c - A) - K_r\dot{A} \quad \text{if } \dot{A} > \dot{A}_m$$

$$T_c = K_p(A_c - A) - K_r\dot{A} + K_i \int^{\text{lim}} (A_c - A)dt \quad \text{if } \dot{A} < \dot{A}_m$$

A = ALTITUDE
A_c = ALTITUDE COMMAND
$\dot{A}_m$ = ALTITUDE RATE THRESHOLD = 0.4 ft/s
T_c = THRUST COMMAND
K_p = PROPORTIONAL GAIN = 0.05
K_r = RATE FEEDBACK GAIN = 0.8
K_i = INTEGRATOR GAIN = 0.001
lim = INTEGRATOR LIMIT = ±1
τ = TIME CONSTANT FOR LOW PASS FILTER - 1.6 s

Figure 16. Hover altitude.

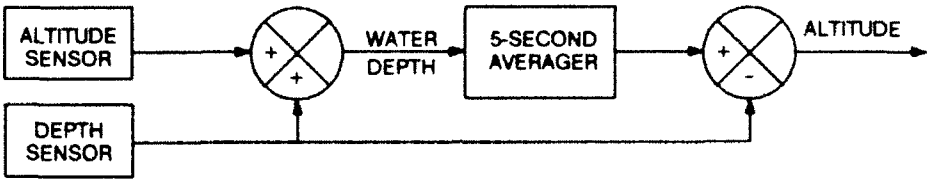

Figure 17. Altitude filter.

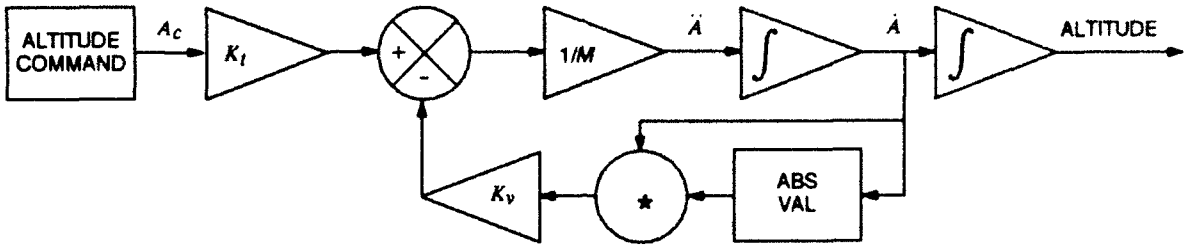

DIFFERENTIAL EQUATION:

$M\ddot{A} + K_v \dot{A}|\dot{A}| = K_t A_c$

A = DEPTH
A_c = DEPTH COMMAND
K_t = THRUST GAIN = 26 lb
K_v = DRAG CONSTANT = 15.2 lb-s^2/ft^2
$1/M$ = 1/MASS = 0.00367 ft/lb-s^2

Figure 18. Hover altitude vehicle dynamics.

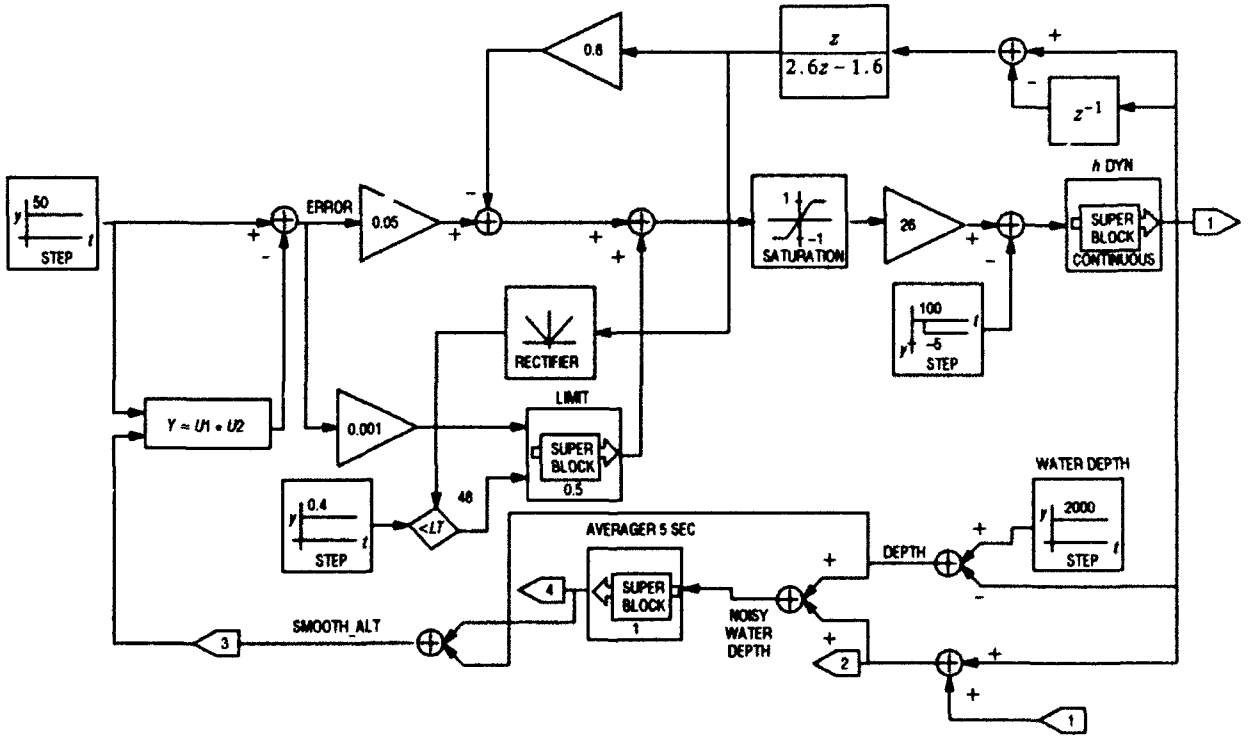

Figure 19. Hover altitude simulation.

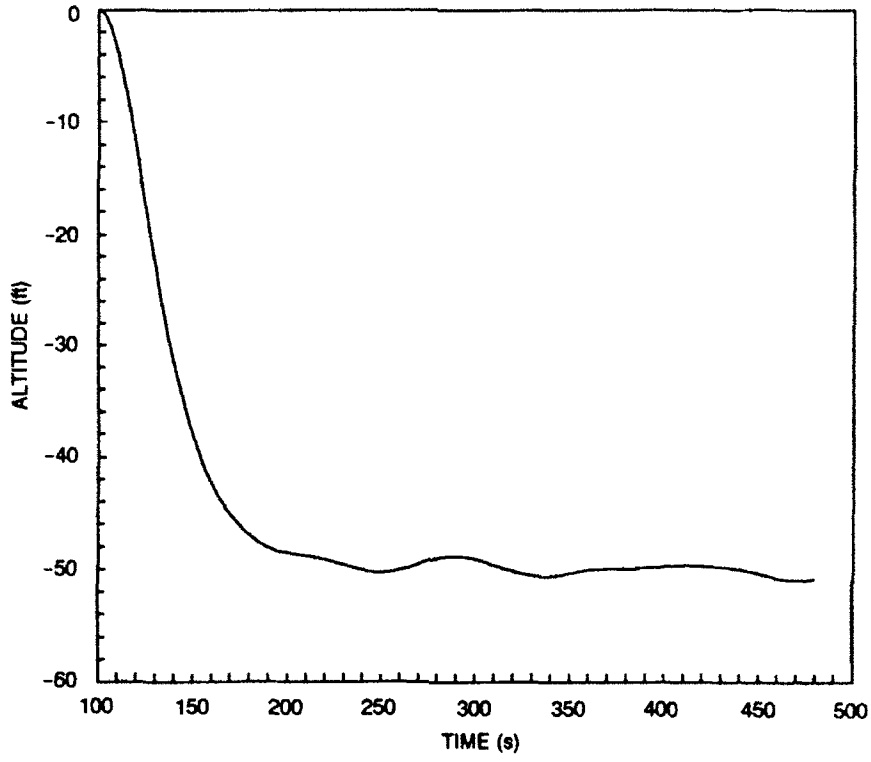

Figure 20. Altitude step response simulation.

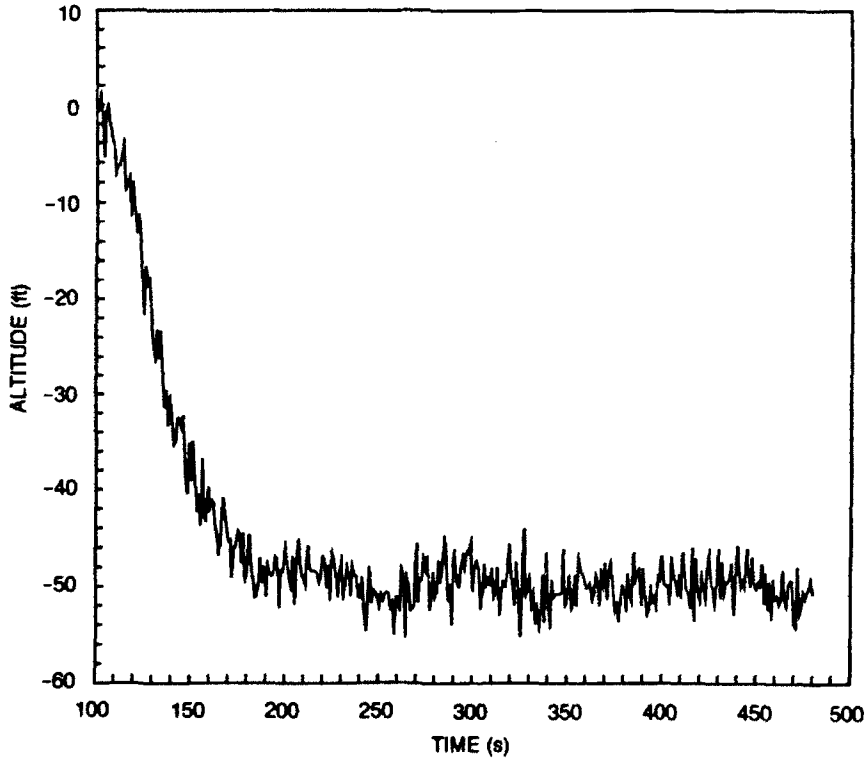

Figure 21. Simulated unfiltered output of the altimeter.

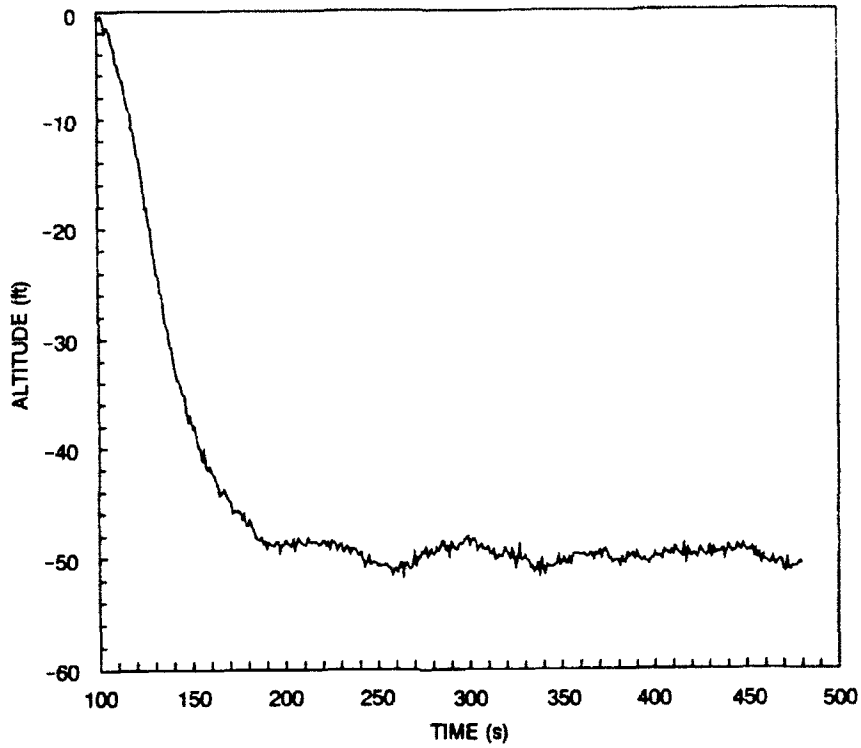

Figure 22. Simulated filtered output of the altimeter.

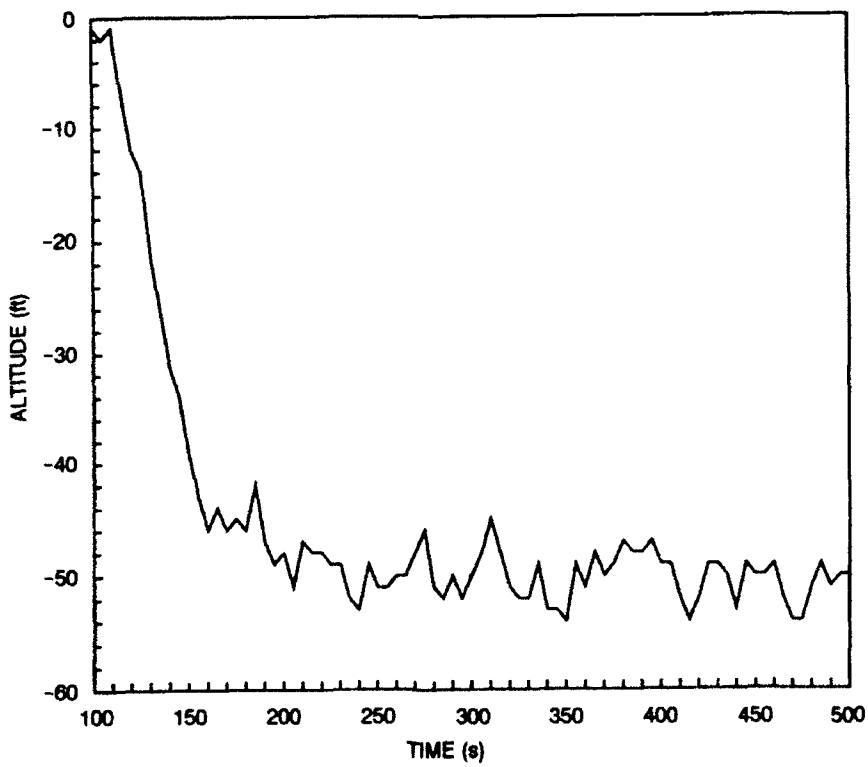

Figure 23. Simulated raw altitude data sampled once every 5 seconds.

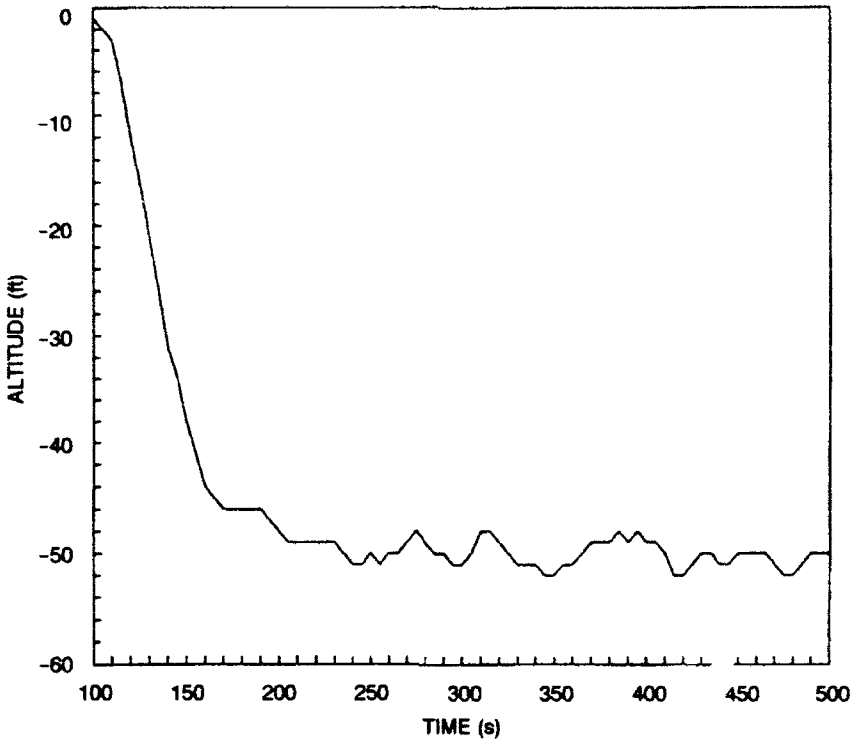

Figure 24. Simulated filtered altitude data sampled once every 5 seconds.

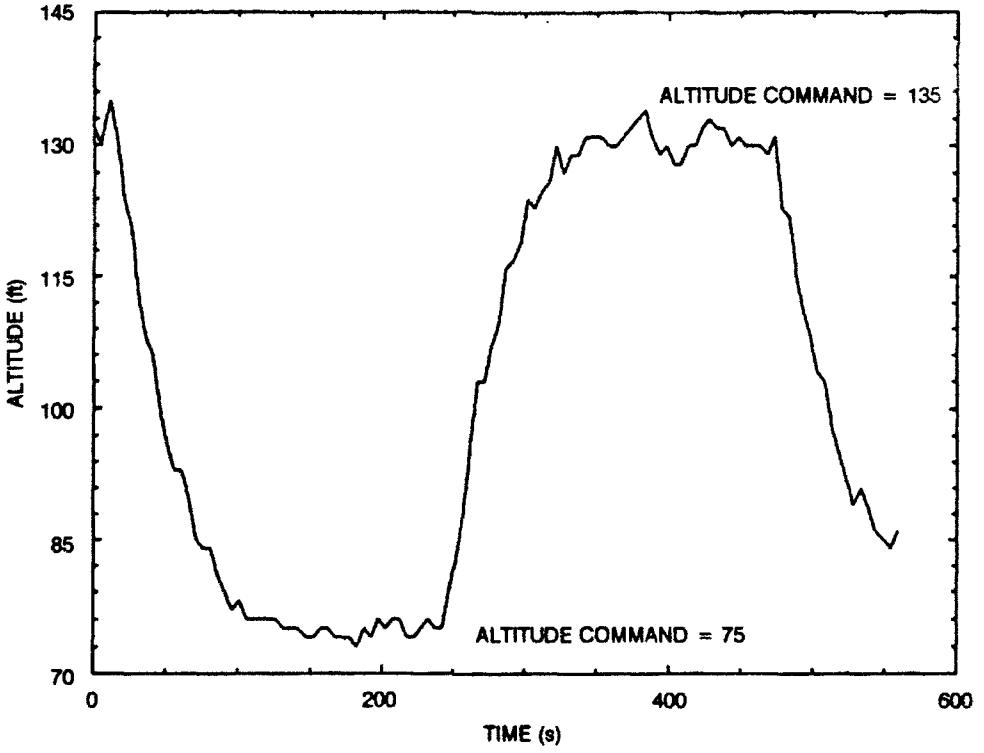

Figure 25. Vehicle hover altitude step response.

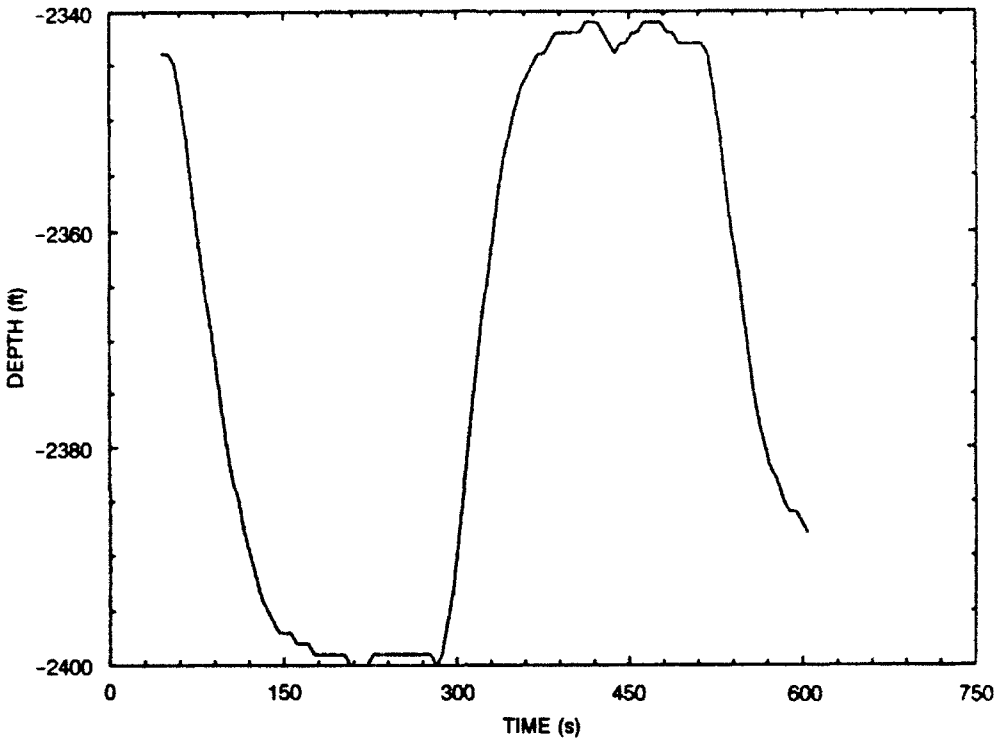

Figure 26. Depth sensor output on altitude step.

BIBLIOGRAPHY

Acoustic Systems, Inc. 1992. "Definition of the Advanced Unmanned Search System (AUSS) Sonar Characteristics." NRaD TN 1704 (Sep). Naval Command, Control and Ocean Surveillance Center, RDT&E Division, San Diego, CA.*

Bryant, S. B. 1979. "Advanced Unmanned Search System (AUSS) Performance Analysis." NOSC TR 437 (Jul). Naval Ocean Systems Center, San Diego, CA.

Cooke, M. W. 1992. "Advanced Unmanned Search System (AUSS)." NRaD TD 2348 (Dec). Naval Command, Control and Ocean Surveillance Center, RDT&E Division, San Diego, CA.

Endicott, D. L. Jr., and G. R. Kuhl. 1992. "Fast Area Search System (FASS): Feasibility Study Appendices." NRaD TN 1703 (Sep). Naval Command, Control and Ocean Surveillance Center, RDT&E Division, San Diego, CA.*

Endicott, D. L. Jr., and G. R. Kuhl. 1992. "The Fast Area Search System (FASS): A Feasibility Study." NRaD TR 1526 (Sep). Naval Command, Control and Ocean Surveillance Center, RDT&E Division, San Diego, CA.

Grace, D. R. 1992. "Brownian Reber Search Theory for the Advanced Unmanned Search System." NRaD TR 1534 (Oct). Naval Command, Control and Ocean Surveillance Center, RDT&E Division, San Diego, CA.

Gunderson, C. R. 1978. "Advanced Unmanned Search System (AUSS), Preliminary Search Systems Analysis." NOSC TR 375 (Dec). Naval Ocean Systems Center, San Diego, CA.

Held, J. L. 1992. "Automatic Hovering Algorithms for the Advanced Unmanned Search System." NRaD TR 1535 (Sep). Naval Command, Control and Ocean Surveillance Center, RDT&E Division, San Diego, CA.

Held, J. L. and H. B. McCracken. 1993. "Automatic Transit Algorithms for the Advanced Unmanned Search System (AUSS)." NRaD TR 1536 (Jan). Naval Command, Control and Ocean Surveillance Center, RDT&E Division, San Diego, CA.

Jones, H. V. 1992. "Advanced Unmanned Search System (AUSS) Description." NRaD TR 1528 (Nov). Naval Command, Control and Ocean Surveillance Center, RDT&E Division, San Diego, CA.

* NRaD Technical Notes (TNs) are working documents and do not represent an official policy statement of the Naval Command, Control and Ocean Surveillance Center (NCCOSC), RDT&E Division (NRaD). For further information, contact the author(s).

Keil, T. J. 1992. "Advanced Unmanned Search System (AUSS) Deep Ocean Floor Search Performance Computer Model: Executive Summary." NRaD TN 1702 (Sep). Naval Command, Control and Ocean Surveillance Center, RDT&E Division, San Diego, CA.*

Kono, M. E. 1992. "Surface Computer System Architecture for the Advanced Unmanned Search System (AUSS)." NRaD TR 1538 (Dec). Naval Command, Control and Ocean Surveillance Center, RDT&E Division, San Diego, CA.

Mackelburg, G. R., S. J. Watson, and W. D. Bryan. 1992. "Advanced Unmanned Search System (AUSS) Acoustic Communication Link Development." NRaD TR 1531 (Nov). Naval Command, Control and Ocean Surveillance Center, RDT&E Division, San Diego, CA.

McCracken, H. B. 1992. "Advanced Unmanned Search System (AUSS) Supervisory Command, Control and Navigation." NRaD TR 1533 (Nov). Naval Command, Control, and Ocean Surveillance Center, RDT&E Division, San Diego, CA.

Osborne, P. D., and C. C. Geurin. 1992. "Advanced Unmanned Search System (AUSS) Surface Navigation, Underwater Tracking, and Transponder Network Calibration." NRaD TR 1532 (Oct). Naval Command, Control and Ocean Surveillance Center, RDT&E Division, San Diego, CA.

Rasmussen, M. E. 1992. "Advanced Unmanned Search System (AUSS) Battery Monitor/Charging Systems." NRaD TR 1539 (Sep). Naval Command, Control and Ocean Surveillance Center, RDT&E Division, San Diego, CA.

Schwager, M., and J. Stangle (SAIC). 1992. "Advanced Unmanned Search System (AUSS) Software Description: Vol I Surface SW/Vol II Vehicle SW." NRaD TN 1705 (Dec). Naval Command, Control and Ocean Surveillance Center, RDT&E Division, San Diego, CA.*

SEACO, Inc. 1992. "Development of the Acoustic Telemetry System." NRaD TD 2336 (Sep). Naval Command, Control and Ocean Surveillance Center, RDT&E Division, San Diego, CA.

Stachiw J. D. 1984. "Graphite-Reinforced Plastic Pressure Hull for the Advanced Unmanned Search System (AUSS) (U)." NOSC TR 999 (Oct). Naval Ocean Systems Center, San Diego, CA.

Stachiw J. D. 1986. "Graphite-Fiber-Reinforced Plastic Pressure Hull Mod 1 for the Advanced Unmanned Search System (AUSS)." NOSC TR 1182 (Dec). Naval Ocean Systems Center, San Diego, CA.

* NRaD Technical Notes (TNs) are working documents and do not represent an official policy statement of the Naval Command, Control and Ocean Surveillance Center (NCCOSC), RDT&E Division (NRaD). For further information, contact the author(s).

Stachiw J. D. 1988. "Graphite-Fiber-Reinforced Plastic Pressure Hull Mod 2 for the Advanced Unmanned Search System (AUSS)." NOSC TR 1245 (Aug). Naval Ocean Systems Center, San Diego, CA.

Uhrich, R. W., J. Walton, and S. J. Watson. 1978. "Portable Test Range and its Application to Side-Looking Sonar." NOSC TR 258 (Jan). Naval Ocean Systems Center, San Diego, CA.

Uhrich, R. W., and S. J. Watson. 1992. "Deep-Ocean Search and Inspection: Advanced Unmanned Search System (AUSS) Concept of Operation." NRaD TR 1530 (Nov). Naval Command, Control and Ocean Surveillance Center, RDT&E Division, San Diego, CA.

Uhrich, R. W., S. J. Watson, and G. R. Mackelburg (Eds.). 1992. "Advanced Unmanned Search System (AUSS) Surface Acoustic Link Description." NRaD TN 1706 (Oct). Naval Command, Control and Ocean Surveillance Center, RDT&E Division, San Diego, CA.*

Vought Corporation. 1992. "Design Analysis and Operations Research for the Advanced Unmanned Search System (AUSS)." NRaD TD 2337 (Sep). Naval Command, Control and Ocean Surveillance Center, RDT&E Division, San Diego, CA.

Walton, J. 1992. "Advanced Unmanned Search System (AUSS) At-Sea Development Test Report." NRaD TR 1537 (Dec). Naval Command, Control and Ocean Surveillance Center, RDT&E Division, San Diego, CA.

Walton, J. 1992. "Advanced Unmanned Search System (AUSS) Testbed: FY 1987 Development Testing." NRaD TR 1525 (Nov). Naval Command, Control and Ocean Surveillance Center, RDT&E Division, San Diego, CA.

Walton, J. 1992. "Advanced Unmanned Search System (AUSS) Testbed: Search Demonstration Testing." NRaD TR 1527 (Nov). Naval Command, Control and Ocean Surveillance Center, RDT&E Division, San Diego, CA.

Walton, J. 1992. "Evolution of a Search System: Lessons Learned with the Advanced Unmanned Search System." NRaD TR 1529 (Nov). Naval Command, Control and Ocean Surveillance Center, RDT&E Division, San Diego, CA.

* NRaD Technical Notes (TNs) are working documents and do not represent an official policy statement of the Naval Command, Control and Ocean Surveillance Center (NCCOSC), RDT&E Division (NRaD). For further information, contact the author(s).

REPORT DOCUMENTATION PAGE

Form Approved
OMB No. 0704-0188

1. AGENCY USE ONLY *(Leave blank)*	2. REPORT DATE	3. REPORT TYPE AND DATES COVERED
	September 1992	Final: Jul 1987–Jun 1992

4. TITLE AND SUBTITLE

AUTOMATIC HOVERING ALGORITHMS FOR THE ADVANCED UNMANNED SEARCH SYSTEM

5. FUNDING NUMBERS

0603713N
S0397
94–MS16–01
DN588521

6. AUTHOR(S)

J. L. Held

7. PERFORMING ORGANIZATION NAME(S) AND ADDRESS(ES)

Naval Command, Control and Ocean Surveillance Center (NCCOSC)
RDT&E Division (NRaD)
San Diego, CA 92152–5000

8. PERFORMING ORGANIZATION REPORT NUMBER

TR 1535

9. SPONSORING/MONITORING AGENCY NAME(S) AND ADDRESS(ES)

Assistant Secretary of the Navy
Research and Development (PMO–403)
Washington, DC 20350

10. SPONSORING/MONITORING AGENCY REPORT NUMBER

11. SUPPLEMENTARY NOTES

12a. DISTRIBUTION/AVAILABILITY STATEMENT

Approved for public release; distribution is unlimited.

12b. DISTRIBUTION CODE

13. ABSTRACT *(Maximum 200 words)*

Certain maneuvering functions of the Advanced Unmanned Search System (AUSS) vehicle must be performed without human intervention. This report covers the design and performance of algorithms for the hovering functions of the AUSS vehicle. The performance of algorithms for hover heading, hover pitch, hover depth, and hover altitude was simulated on a computer and measured by at-sea testing. This report documents that performance.

14. SUBJECT TERMS

deep ocean search
hovering algorithms
hover heading
hover depth
hover pitch
hover altitude
AUSS
Advanced Unmanned Search System
vehicle dynamics

15. NUMBER OF PAGES

29

16. PRICE CODE

17. SECURITY CLASSIFICATION OF REPORT	18. SECURITY CLASSIFICATION OF THIS PAGE	19. SECURITY CLASSIFICATION OF ABSTRACT	20. LIMITATION OF ABSTRACT
UNCLASSIFIED	UNCLASSIFIED	UNCLASSIFIED	SAME AS REPORT

21a NAME OF RESPONSIBLE INDIVIDUAL	21b TELEPHONE (Include Area Code)	21c OFFICE SYMBOL
J. L. Held	(619) 553-1889	Code 941